A study on airflow resistivity models for multi-component polyester fiber assembly

Tao Yang[a*], Rajesh Mishra[a], Kirill V Horoshenkov[b], Alistair Hurrell[b], Ferina Saati[c] and Xiaoman Xiong[a]

[a]*Department of Material Engineering, Faculty of Textile Engineering, Technical University of Liberec, Liberec 46117, Czech Republic*

[b]*Department of Mechanical Engineering, The University of Sheffield, Sheffield S1 3JD, United Kingdom*

[c]*Department of Mechanical Engineering, Technical University of Munich, Boltzmannstrasse 15, 85748 Garching, Germany*

Abstract
The airflow resistivity is a key parameter to predict accurately the acoustical properties of fibrous media. There is a large number of theoretical and empirical models which can be used to predict the airflow resistivity of this type of porous media. However, there is a lack of experimental data on the accuracy of these models in the case of multi-component fibrous media. This paper presents a detailed analysis of the accuracy of several existing models to predict airflow resistivity which make use of the bulk density and mean fibre diameter information. Three types of polyester (PET) materials made using regular PET, hollow PET and bi-component PET with a range of densities are chosen for this study. It is shown that some existing models largely under- or overestimate the airflow resistivity when compared with the measured values. A novel feature of this work is that it studies the relative performance of airflow resistivity prediction models that are based on the capillary channel theory and drag force theory. These two groups of models are then compared to some purely empirical models. It is found that the prediction error by some models is unacceptably high (e.g. >20-30%). The results suggest that there are existing models which can predict the airflow resistivity of multi-component fibrous media with 8-10% accuracy.

keywords: Airflow resistivity, multi-component fibre, nonwoven, polyester, acoustical properties

---

* Corresponding author at: Department of Material Engineering, Faculty of Textile Engineering, Technical University of Liberec, Liberec 46117, Czech Republic.
E-mail address: tao.yang@tul.cz

1. Introduction

The airflow resistivity is one of the most critical parameters determining the sound absorption properties of a porous absorber. It is a measure of how easily air can enter a porous absorber and the resistance that airflow meets within a structure. Once the airflow resistivity is known, a series of theoretical or empirical models can be applied to predict the impedance and absorption coefficient of fibrous media [1]. The values of airflow resistivity vary largely between various type of common porous absorbent materials. It therefore gives some sense of how much sound energy may enter the material pores to be lost due to viscous and inertia effects. According to the direct airflow method detailed in the standard ISO 9053-1991 [2], the airflow resistivity is determined by an experiment where a sample of a porous material is placed in a tube, and a steady airflow is passed through the sample. The airflow velocity, u, the pressure drop between two sides of the sample, Δp, and the thickness of the sample, h, are measured [2]. The airflow resistivity, σ, of the material is then defined:

$$\sigma = \frac{\Delta p}{uh}, \qquad (1)$$

Polyester fiber materials are innovative products which are becoming widespread sound absorbers. These recyclable and long lasting materials are replacing traditional glass wool and rock wool in many noise control applications. Traditionally, polyester fiber materials used in sound absorption applications were manufactured from mono-size fibres or single-component fibrous materials, i.e. materials composed of fibres with identical or similar diameter and shape. Recently, multi-component polyester materials have started to become more popular replacing single component polyester materials. However, there is limited amount of data on the acoustical and related non-acoustical properties of multi-component polyester materials [3]. Therefore, the major objective of this study is to measure the airflow resistivity for a representative range of fibrous media and use data to understand better the effect of fiber diameter distribution on the accuracy of model predictions.

2. Review of previous works on airflow resistivity models

There are a large number of theoretical and empirical models to predict the airflow resistivity for fibrous and granular media. Good reviews of some of these models can be found in refs. [4-6]. These models can be grouped into two main categories: theoretical models and empirical models. In this section, the previous works on airflow resistivity models will be introduced and we will review mathematical expressions from some existing models for the airflow resistivity for completeness. In section 3 we will use these models to predict the measured flow resistivity of multi-component polyester fibre.

2.1. Theoretical models

There are two main theories in airflow resistivity theoretical models: capillary channel theory and drag force theory. The airflow resistivity models established using capillary channel theory are based on the works of Hagen-Poiseuille, Kozeny and Carman, where the flow through the porous material is treated as a conduit flow between parallel cylindrical capillary tubes [7,8]. Davies presented a model to fit his own transverse permeability data for the flow through porous fibrous materials having a high fabric porosity (as high as 0.7) [9]. The airflow resistivity of fiber orientation along the flow direction was in the same form as the Kozeny-Carman equation, and the airflow resistivity of fiber orientation perpendicular to the flow

direction was obtained using the lubrication approximation, assuming that the narrow gaps between adjacent cylinders dominate the flow resistance [10,11]. Pelegrinis *et al.* modified the Kozeny-Carmen model to obtain more accurate prediction for the airflow resistivity of uniform fiber diameter polyester material [12]. Lind-Nordgren and Göransson presented a scaling law applied to the airflow resistivity of porous materials having a porosity and tortuosity close to 1 [13]. However, it has been argued that those models based on capillary channel theory can be unsuitable for high porosity media in which the porosity is greater than 0.8 [8]. Airflow resistivity models based on capillary channel theory are summarized in Table 1.

Table 1
Airflow resistivity models established using capillary channel theory.

Method	Airflow resistivity
Davies CN [9]	$\sigma = \dfrac{64\eta(1-\varepsilon)^{1.5}[1+56(1-\varepsilon)^3]}{d^2}$
Kozeny-Carman [8]	$\sigma = \dfrac{180\eta(1-\varepsilon)^2}{d^2\varepsilon^3}$
Lind-Nordgren [13]	$\sigma = \dfrac{128\eta(1-\varepsilon)^2}{d^2\varepsilon}$
Doutres *et al.* [14]	$\sigma = \dfrac{128\eta(1-\varepsilon)^2}{d^2}$
Pelegrinis *et al.* [12]	$\sigma = \dfrac{180\eta(1-\varepsilon)^2}{d^2}$

Note: η is the air dynamic viscosity, ε is the material porosity and d is the fiber diameter.

There are also a number of airflow resistivity models which are based on drag force theory. In these models the fibers in the porous material that form the walls of the pores in the structure, are treated as obstacles to a straight flow of the fluid and it is assumed that the frame is rigid and that the fibers cannot be displaced [15]. The sum of all the 'drags' is assumed to be equal to the total resistance to flow in the porous material. Unlike capillary flow theory, drag force theory and unit cell models demonstrate the relationship between permeability and the internal structural architecture of the porous material. In drag force models, the fibers are assumed to be aligned unidirectionally in a periodic pattern such as a square, triangular or hexagonal array. The airflow resistivity of unidirectional fibrous materials can then be solved using the Navier-Stokes equation in the unit cell with appropriate boundary conditions [4]. One of the earliest equivalent dimensionless permeability for flow parallel to an array of fibres was developed by Langmuir [16]. Tarnow presented a new way to calculate the airflow resistivity of randomly placed parallel fibers based on Voronoi polygons [17]. In his study, Tarnow discussed a two-dimensional model consisting of parallel fibers randomly spaced for flow parallel and perpendicular to the fibers.. A summary of these models is given in Table 2.

Table 2
Airflow resistivity models established using drag force theory.

Method	Airflow resistivity
Langmuir [16]	$\sigma = \dfrac{16\eta(1-\varepsilon)}{d^2[-\ln(1-\varepsilon)-1.5+2(1-\varepsilon)-\frac{(1-\varepsilon)^2}{2}]}$
Hasimoto [18]	$\sigma = \dfrac{32\eta(1-\varepsilon)}{d^2(-\ln(1-\varepsilon)-1.476)}$
Kuwabara [19]	$\sigma = \dfrac{32\eta(1-\varepsilon)}{d^2[-\ln(1-\varepsilon)-1.5+2(1-\varepsilon)-\frac{(1-\varepsilon)^2}{2}]}$

Happel [20]

A. Flow parallel to fibers

$$\sigma = \frac{72\eta(1-\varepsilon)}{d^2[-\ln(1-\varepsilon) - 3 + 4(1-\varepsilon) - (1-\varepsilon)^2]}$$

B. Flow perpendicular to fibers

$$\sigma = \frac{72\eta(1-\varepsilon)}{d^2[-\ln(1-\varepsilon) - \frac{1-(1-\varepsilon)^2}{1+(1-\varepsilon)^2}]}$$

Tarnow [17]

Flow parallel to fibers

A. Square lattice

$$\sigma = \frac{16\eta(1-\varepsilon)}{d^2[-\ln(1-\varepsilon) + 0.5 - 2\varepsilon]}$$

B. Random lattice

$$\sigma = \frac{16\eta(1-\varepsilon)}{d^2[-1.280\ln(1-\varepsilon) + 0.526 - 2\varepsilon]}$$

Flow perpendicular to fibers

C. Square lattice

$$\sigma = \frac{16\eta(1-\varepsilon)}{d^2\{\ln[(1-\varepsilon)^{-1/2}] - 0.5\varepsilon - 0.25\varepsilon^2\}}$$

D. Random lattice

$$\sigma = \frac{16\eta(1-\varepsilon)}{d^2[-0.640\ln(1-\varepsilon) + 0.263 - \varepsilon]}$$

2.2. Empirical models

An empirical model of airflow resistivity was first introduced by Nichols, who suggested that the flow resistance, $\sigma h \sim (\rho h)^{1+x} / d^2$, where the adjustable parameter is $0.3 \leq x \leq 1$. This parameter value depends on the distribution of the fibers in material [21]. Based on the work by Nichols, Bies and Hansen presented a simple model which allows the calculation of the airflow resistivity of fibreglass starting from the values of its bulk density and fiber diameter [22]. Garai and Pompoli investigated the airflow resistivity of double fiber component polyester materials and extended the Bies and Hansen model to predict the flow resistivity of polyester fibres [23]. Manning and Panneton analyzed the acoustic behavior of shoddy fiber materials manufactured by three different methods: mechanical bonding, thermal bonding, and resin bonding. They established three simple airflow resistivity models based on weight-of-evidence approach [24]. A summary of the equations for these empirical models is given in Table 3.

Table 3
Airflow resistivity models established using empirical method.

Method	Airflow resistivity	
Bies & Hansen [22]	$\sigma = \dfrac{3.18 \times 10^{-9}\rho^{1.53}}{d^2}$	
Garai & Pompoli [23]	$\sigma = \dfrac{2.83 \times 10^{-8}\rho^{1.404}}{d^2}$	
Manning & Panneton [24]	Mechanically bonded	$\sigma = \dfrac{2.03\times10^{-8}\rho^{1.485}}{d^2}$
	Resin bonded	$\sigma = \dfrac{3.61\times10^{-9}\rho^{1.804}}{d^2}$
	Thermally bonded	$\sigma = \dfrac{1.94\times10^{-8}\rho^{1.516}}{d^2}$

3. Materials and Methods

One polyester nonwoven material prepared by vibrating perpendicular technology [25] at the Technical University of Liberec, Czech Republic, as well as two types of commercially available polyester nonwoven materials which were separately made by vibrating perpendicular technology and rotating perpendicular technology were selected for this study. Sample WM was prepared by rotating perpendicular technology; samples ST T1 and ST T2 were produced by vibrating perpendicular technology [26]. Fig. 1. (a) is photographs which illustrate the dominant angle of fibre orientation of samples WM, ST T1 and ST T2. In this study, the fibre orientation angle was defined as the angle between the dominant fibre axis (see areas in Fig. 1(a) highlighted in green) and the surface of the material specimen. This angle was dependent on the degree of compression/material density in the fibrous specimen. Fig. 1 (b) shows scanning electron microscope image of sample WM taken at 200x magnification. The latter is one of 150 collected SEM images which were used to analyze fiber diameter distribution.
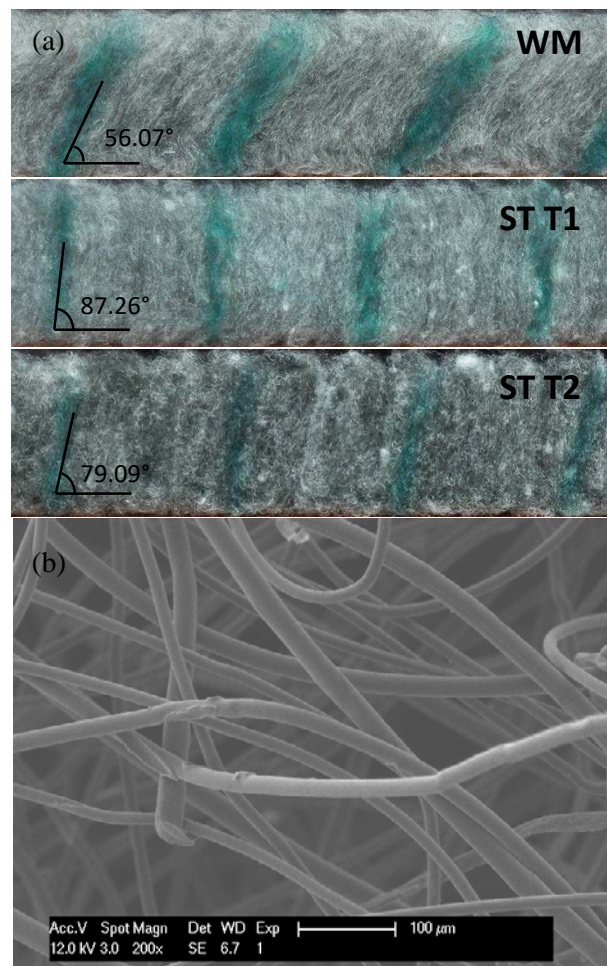

Fig. 1. Cross-sectional macroscopic images of samples WM, ST T1 and ST T2 (a) and the scanning electron microscope (SEM) image of sample WM (b).

In order to produce polyester material samples with different thicknesses and densities, the heat-pressing method was applied. Samples WM, ST T1, and ST T2 were compressed under 600 Pa pressure at 130 °C for 5 min. Thickness gauges were applied to measure the thickness attained in this process. The characteristics of the polyester specimens are listed in Table 4. All of the samples in this study have the same fiber content. The sheath part of bi-component fibers

is low-melting polyethylene terephthalate (PET). The polyester materials were made of three types of polyester fibers. The resin embedding technology was used to get the cross-sectional slice of fibers, microscope was then applied to get the cross-sectional microscopic images (see in Fig. 2). The content percentage of samples is based on weight. Fabric thicknesses were measured with an Alambeta device (SENSORA, Liberec, Czech Republic). Fabric areal density was determined according to ISO 9073-1:1989 [27]. Sample porosities were determined according to ASTM C830-00 [28]. The voids in hollow fibers were not included in the analysis, because these closed pores have little or no effect on the airflow flow resistivity and sound absorption (e.g. [29]). In terms of fibre orientation, it can be seen that a majority of fibres in an uncompressed sample are vertically orientated and parallel arranged as illustrated in Fig. 1. (a). The fibre orientation angle decreased during the heat-pressing process that resulted in a reduced specimen thickness and increased material density.

100 mm diameter circular shape samples were cut with an ELEKTRONISCHE STANZMASCHINE TYPE 208 machine to measure the airflow resistivity using a standard setup. In the present study, the airflow resistivity was measured with an AFD300 AcoustiFlow device (The Gesellschaft für Akustikforschung Dresden mbH, Dresden, Germany) according to ISO 9053:1991 [2]. Ten samples were measured for each polyester nonwoven fabric to study the reproducibility of the airflow resistivity experiment and scattering in the obtained data. The results are summarized in Table 4. The relative density quoted in Table 4 was calculated as the ratio of the material bulk density, ρ, to the fibre density, ρ_f, i.e. ρ / ρ_f, where the value of the fibre density set to 876.53 kg/m^3. A relatively low fibre density is explained by a relatively high proportion of hollow fibres in the mixture. The flow resistivity is plotted against this parameter in section 4.

Table 4
Characteristics of polyester materials.

| Samples	Fiber contents	Mean fiber diameter (μm)	Porosity (%)	Relative density (%)	Bulk density (kg/m^3)	Thickness (mm)	Surface density (g/m^2)	Airflow resistivity (Pa·s/m²)	Fibre orientation angle (°)
WM			97.60	2.40	21.07	24.09	507.5	5757 ± 589	56.07
WM			97.21	2.79	24.45	20.76	507.5	7319 ± 243	45.65
WM			96.95	3.05	26.71	19.00	507.5	8630 ± 408	40.88
WM			96.86	3.14	27.54	18.43	507.5	10329 ± 376	39.41
WM			95.94	4.06	35.56	14.27	507.5	14990 ± 285	29.44
WM	30%-		95.91	4.09	35.87	14.15	507.5	15410 ± 167	29.17
WM	Hollow		94.80	5.20	45.56	11.14	507.5	22230 ± 433	22.56
ST T1	PET		98.08	1.92	16.87	28.36	478.3	4011 ± 316	87.26
ST T1	45% ii-	18.65	97.31	2.69	23.54	20.32	478.3	7498 ± 332	45.70
ST T1	PET		97.20	2.80	24.54	19.49	478.3	7412 ± 328	43.35
ST T1	25% iii-		96.47	3.53	30.94	15.46	478.3	13400 ± 277	32.99
ST T1	Bi-		95.79	4.21	36.88	12.97	478.3	16750 ± 442	27.18
ST T2	componen		98.07	1.93	16.93	27.48	465.2	4108 ± 199	79.09
ST T2	t PET		97.78	2.22	19.49	23.87	465.2	5337 ± 217	58.53
ST T2			97.44	2.56	22.48	20.69	465.2	7029 ± 356	47.67
ST T2			96.85	3.15	27.61	16.85	465.2	10180 ± 259	37.02
ST T2			96.01	3.99	34.95	13.31	465.2	13370 ± 199	28.40
ST T2			94.91	5.09	44.60	10.43	465.2	20470 ± 687	21.88

PET: polyethylene terephthalate.
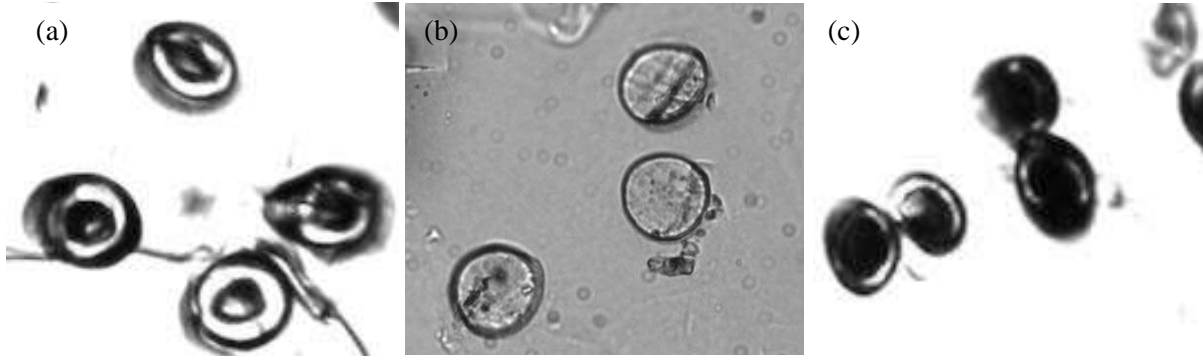
Fig. 2. Cross-sectional microscopic pictures of polyester fibers: (a) hollow PET; (b) PET; (c) bicomponent PET.

The fiber diameter was required to predict the airflow resistivity with a theoretical model. In this study, the polyester nonwoven materials were made with three types of fiber. The fiber diameter has been determined using the ImageJ software based on the scanning electron microscope (SEM) images (see Fig. 1. (b)), so that the fiber diameter distribution for polyester nonwovens were obtained. 2358 fiber diameters from 150 SEM images were measured in total to ensure reproducible statistics. The fiber diameter distribution is shown in Fig. 3. The kernel density estimation was applied to get the distribution line in the image analysis. Obviously, some of the features are that it has at least two peaks and one tail at the large diameter end. A symmetric fiber diameter distribution on either side of the highest peak implies that the finest fiber is the key component which is 45% in polyester materials. An asymmetric fiber diameter distribution can be found at the second peak from the left and the slope of distribution line has a slight decrease after the peak. It indicates that there is another type of polyester fiber besides the two types of fiber which can be easily distinguished from the first and second peaks from the left. Thus, samples have triple fiber components with rough diameter of 13, 19 and 22 μm. The mean fiber diameter of multi-component polyester materials was determined according to the following equation:

$$d = \frac{\sum_{i=1}^{n} d_i}{n} \ ,$$

(2)

where n is the total fiber count, d_i is the diameter for each fiber. The mean diameter of polyester fibres was presented in Table 4.
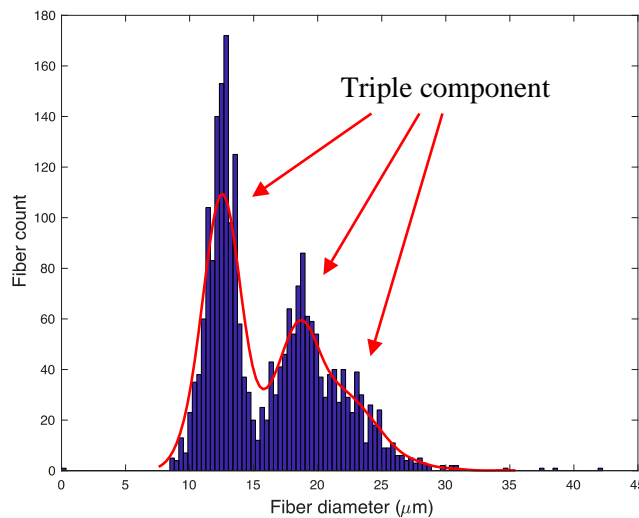
Fig. 3. Fiber diameter distribution of polyester nonwovens WM, ST T1 and ST T2 obtained for 2358 fiber diameter data.

4. Results and discussion

The accuracy of the airflow resistivity prediction models presented in Tables 1-3 was compared against the obtained experimental data. The accuracy of theoretical and empirical models was investigated by comparing the relative prediction errors. In this calculations the values of the material density, porosity and mean fibre diameter were taken from Table 4. In order to investigate the accuracy of airflow resistivity models, the relative prediction error was calculated according to the following equation:

$$\Delta = \frac{\sum_{n=1}^{N} \Delta_n}{N} = \frac{1}{N}\sum_{n=1}^{N}\frac{|\sigma_{p,n}-\sigma_{m,n}|}{\sigma_{m,n}} \quad , \tag{3}$$

where σ_p is the predicted airflow resistivity, σ_m is the measured airflow resistivity, and N is the total number of material specimens studied (N=18). A relative error of 0.2 means a difference of 20% from the measured value.

4.1. Prediction of airflow resistivity based on theoretical models

Due to the same fiber content in samples WM, ST T1 and ST T2 the airflow resistivity was descried as a function of relative density which was determined as a ratio of the material density over the density of polyester. The predicted airflow resistivity values based on capillary channel theory (see the models listed in Table 1) are show in Fig. 4. (a) as a function of the relative density. The relative prediction errors of capillary channel theory models are compared in Fig. 4. (b). It can be seen that Doutres and Lind-Nordgren models predict similar values of the airflow resistivity. The Kozeny-Carman model agrees closely with that by Pelegrinis *et al*. This difference can be explained by the fact that the two sets of models make use of rather different coefficients in the flow resistivity equations: 180 for the Kozeny-Carman type models; and 128 for the Lind-Nordgren models. This difference in the predicted airflow resistivity increases proportional to the material density. The Davies CN model shows the highest value of predicted airflow resistivity and a relatively high error. It is observed that the maximum relative error for this model is 98.8%. The relative error of Kozeny-Carman model is relatively low, with a maximum value of 12.3%. The maximum error for the Pelegrinis *et al.* model is 8.4% which is the lowest among the five models considered. It was also found that the Pelegrinis *et al.* model is more reliable when the material density is relatively low. However, it begins to overestimate the airflow resistivity as the relative density increases above 4%.
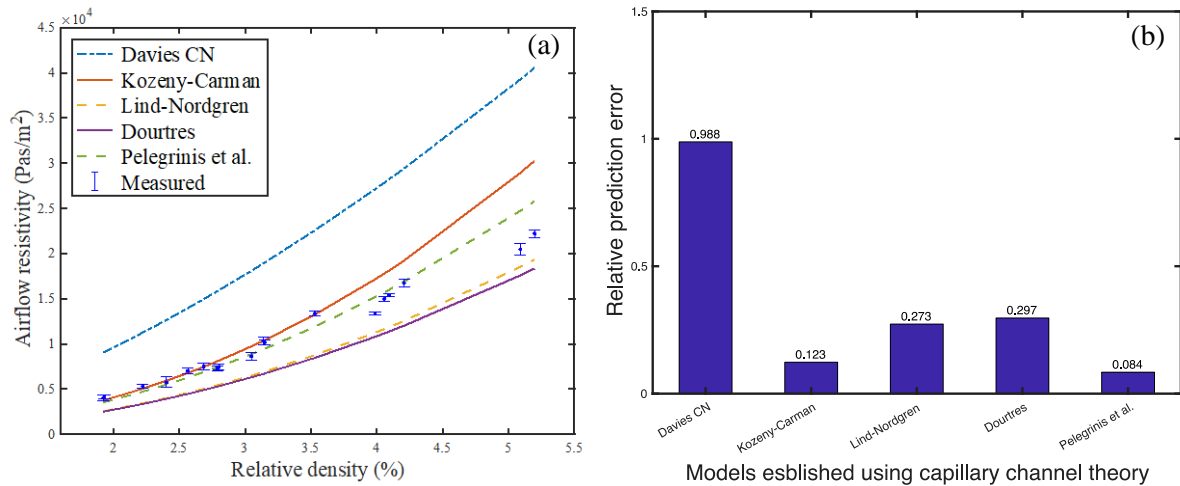
Fig. 4. (a) Predicted airflow resistivity based on capillary channel theory and (b) the prediction error of airflow resistivity.

The calculated airflow resistivity of multi-component polyester materials based on the drag force theory is presented in Fig. 5 (a) as a function of the relative density. Fig. 5 (b) presents the predicted errors. The keys to the model type can be found in Table 2. The results presented in Fig. 5 suggest that the model by Happel (Happel B model) for the airflow perpendicular to fibres significantly overestimate the resistivity by over 400%. The predictions by Hasimoto, Kuwabara, Happel A (airflow parallel to the fibers) and Tarnow C (airflow perpendicular to fibers arranged in the form of lattice) are very similar and overestimate the measured airflow resistivity by 180-210%. The predictions by the Langmuir and Tarnow A (airflow parallel to the fibres arranged in square lattice) are almost identical but overestimate the airflow resitivity by approximately 40%. The predictions by Tarnow D model (airflow is perpendicular to the fibres arranged in random lattice) fall between the two latter groups. The most accurate model for the flow resistivity of this kind of fibres is the Tarnow B model (airflow is parallel to fibres arranged in random lattice). This model is accurate within 10%. In addition, it can be seen that the Tarnow B model is more accurate when the materials have relatively low density, however this model exhibits higher variation comparing to measured values at high density range. This phenomenon can be explained by the decrease of fibre orientation angle with increased density for high specimen compression as illustrated in Fig. 1(a). When the fibre orientation angle decreases, the airflow is no longer parallel to the fibres. When the orientation angle is close to 0 the airflow becomes perpendicular to the fibres. For these materials the measured flow resistivity (see Fig. 5 (a)) is higher than that predicted with Tarnow A and B models which work better when the flow is parallel to the fibres.
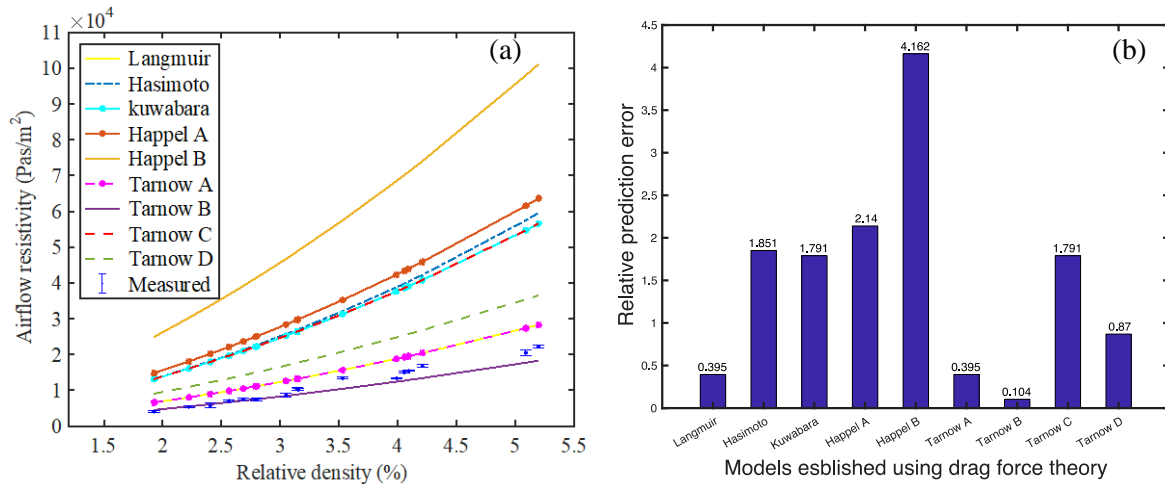
Fig. 5. (a) Predicted airflow resistivity based on drag force theory and (b) the prediction error of airflow resistivity. See Table 2 for the key to the model type.

4.2. Prediction of airflow resistivity using empirical models

The predicted airflow resistivity calculated from empirical models are presented in Fig. 6. (a). Fig. 6 (b) presents the prediction error data. The Bies-Hansen and Manning RB models give significantly underestimated airflow resistivity of multi-component polyester materials in comparison with measured values. This can be explained by the different materials and bonding method in their studies in comparison with in the current study [22, 24]. Garai, Manning MB and TB models exhibit similar results and relative good agreement by comparing the measured airflow resistivity. It is observed that the prediction errors for these three models range from 11.1% to 15.7%. The predictions by Manning TB and Garai are very close, but Manning TB method shows better predictions. The relative error for Manning RB/TB and Garai models increase with the increased value of the relative density. The relative error for these models is below 10% when the relative density of the fibrous material is below 3%.
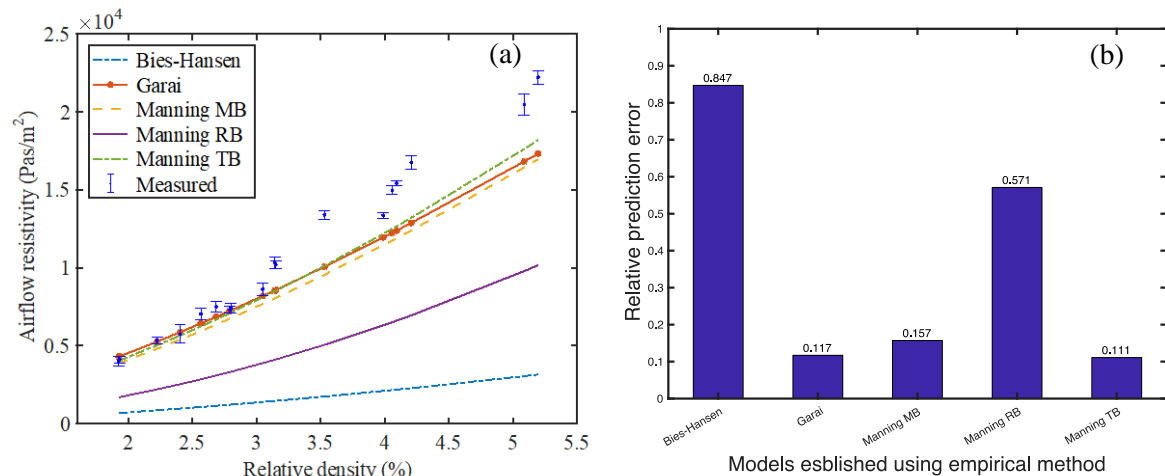

Fig. 6. (a) Predicted airflow resistivity based on empirical models and (b) the prediction error of airflow resistivity. MB is mechanically bonded; RB is resin bonded; TB is the thermally bonded.

5. Conclusions

This work has studied the accuracy of commonly used airflow resistivity models for fibrous media. Those models have been grouped into two main categories: theoretical and empirical. In order to select the most reliable models for multi-component polyester materials, three types of polyester nonwoven samples were developed and studied with the relative density being in the range of 1.92 – 5.2%. The fiber diameter distribution was obtained using ImageJ software with mean fibre diameter being 18.65 μm. The airflow resistivity results have been carried out by AFD300 Acoustic Flow device. The effect of the fibre orientation angle on the flow resistivity of fibrous specimens was also studied. As expected, the flow resistivity increases with the decreased fibre orientation angle, i.e. when the flow becomes perpendicular to the fibres. However, this effect was found to be relatively small in comparison with the effect of material density. The error between predicted and measured airflow resistivity has been determined. The results indicate that the Pelegrinis *et al.* model is the most suitable model for multi-component polyester material in those models established using capillary channel theory, and the relative prediction error is 8.43% for this class of fibrous media. For models based on drag force theory, one of the Tarnow models exhibits relatively high accuracy with a relative prediction error of 10.41%. It is observed that some existing empirical models are acceptable for multi-component polyester materials. One of the Manning model exhibits good agreement with the value of measured airflow resistivity, the prediction error is 11.1%.

Acknowledgment

References:

[1] Ingard U. Notes on Sound Absorption Technology, Noise Control Foundation, New York, 1994.

[2] ISO 9053-1991: Acoustics -- Materials for acoustical applications -- Determination of airflow resistance.

[3] Luu HT, Perrot C, Panneton R. Influence of porosity, fiber radius and fiber orientation on the transport and acoustic properties of random fiber structures. Acta Acust United Ac 2017; 103: 1050-1063.

[4] Tang X, Yan X, Acoustic energy absorption properties of fibrous materials: A review. Composites Part A 2017; 101: 360-380.

[5] Luu HT, Perrot C, Monchiet V, Panneton R. Three-dimensional reconstruction of a random fibrous medium: Geometry, transport, and sound absorbing properties. J Acoust Soc Am 2017; 141: 4768-4780.

[6] Xue Y, Bolton JS. Prediction of Airflow Resistivity of Fibrous Acoustical Materials Having Double Fiber Components and a Distribution of Fiber Radii. Proceedings of International Congress on Noise Control Engineering 2017, Hong Kong.

[7] Sutera SP, Richard S. The History of Poiseuille's Law. Annu Rev Fluid Mech 1993; 25: 1–20.

[8] Carman PC. Flow of Gases through Porous Media. New York: Academic Press, 1956.

[9] Davies CN. The Separation of Airborne Dust and Particles. Proceedings of the Institution of Mechanical Engineers, Part B: Management and Engineering Manufacture 1953; 1: 185–213.

[10] Carman PC. Fluid Flow through Granular Beds. Chem Eng Res Des 1997; 75: 32–48.

[11] Chen X. Modelling and Predicting Textile Behaviour. Woodhead Publishing Series in Textiles, no. 94. Cambridge: Boca Raton, Fla: Woodhead Publishing: In association with the Textile Institute; CRC Press, 2010.

[12] Pelegrinis MT, Horoshenkov KV, Burnett A. An Application of Kozeny–Carman Flow Resistivity Model to Predict the Acoustical Properties of Polyester Fibre. Appl Acoust 2016; 101: 1–4.

[13] Lind-Nordgren E, Göransson P. Optimising Open Porous Foam for Acoustical and Vibrational Performance. J Sound Vib 2010; 329: 753–67.

[14] Doutres O Atalla N, Dong K. Effect of the Microstructure Closed Pore Content on the Acoustic Behavior of Polyurethane Foams. J Appl Phys 2011; 110: 064901.

[15] Scheidegger AE. THE PHYSICS OF FLOW THROUGH POROUS MEDIA, Adrian E.: University of Toronto Press, Toronto Hardcover, 2nd Edition, 1963.

[16] Langmuir I. Report of Smokes and Filters, Part IV of a report for the Office of Scientific Research and Development, OSRD No. 865, Ser. No. 353, Filtration of Aerosols and the Development of Filter Materials, by Rodebush, W. H. et al., September 4, 1942.

[17] Tarnow V. Airflow Resistivity of Models of Fibrous Acoustic Materials. J Acoust Soc Am 1996; 100: 3706–3713.

[18] Hasimoto H. On the Periodic Fundamental Solutions of the Stokes Equations and Their Application to Viscous Flow Past a Cubic Array of Spheres. J Fluid Mech 1959; 5: 317-328.

[19] Kuwabara S. The Forces Experienced by Randomly Distributed Parallel Circular Cylinders or Spheres in a Viscous Flow at Small Reynolds Numbers. J Phys Soc Jpn 1959; 14: 527-532.

[20] Happel J. Viscous Flow Relative to Arrays of Cylinders. AIChE J 1959; 5: 174-177.

[21] Nichols RH. Flow-Resistance Characteristics of Fibrous Acoustical Materials. J Acoust Soc Am 1947; 19: 866–71.

[22] Bies DA, C Ho Hansen. Flow Resistance Information for Acoustical Design. Appl Acoust 1980; 13: 357–391.

[23] Garai M, Pompoli F. A Simple Empirical Model of Polyester Fibre Materials for Acoustical Applications. Appl Acoust 2005; 66: 1383–1398.

[24] Manning J, Panneton R. Acoustical Model for Shoddy-Based Fiber Sound Absorbers. Text Res J 2013; 83: 1356–70.

[25] Jirsak O, Wadsworth L. Nonwoven Textiles. Durham, NC: Carolina Academic Pr, 1998.

[26] Yang T, Xiong X, Mishra R, Novák J, Militký J. Sound Absorption and Compression Properties of Perpendicular-Laid Nonwovens. Text Res J 2018. doi: 10.1177/0040517517753634.

[27] ISO 9073-1:1989. Textiles -- Test methods for nonwovens -- Part 1: Determination of mass per unit area.

[28] ASTM C830-00: 2000. Standard test methods for apparent porosity, liquid absorption, apparent specific gravity, and bulk density of refractory shapes by vacuum pressure.

[29] McRae JD, Naguib HE, Atalla N. Mechanical and Acoustic Performance of Compression-Molded Open-Cell Polypropylene Foams. J Appl Polym Sci 2010; 116: 1106–1115.